Joshua R. Uzarski, Charlene M. Mello

US Army Natick Solider Research, Development, and Engineering Center

Natick, MA 07160

University of Massachusetts Dartmouth

Chemistry and Biochemistry Department

North Dartmouth, MA 02747

Detection and classification of related lipopolysaccharides via a small array of immobilized antimicrobial peptides

The following supplemental information provides further detailed experimental and analysis procedures. Experimental data is presented supporting the mathematical treatment of lipopolysaccharide binding data to immobilized antimicrobial peptides via surface plasmon resonance. More detailed data tables resulting from linear discriminant analysis calculations are presented to support the data presented in the main text. A detailed explanation of the surface-dependent properties of the immobilized antimicrobial peptides is offered.

Table of Contents

S1. Surface Derivitization Reactions for RAIRS characterization S-2

S2. Peptide Immobilization on SPR Substrates S-2

S3. LPS Binding S-3

S4. Correction for Peptide Binding Affinity Decay S-4

S5. Peptide-LPS Binding Decay Correction Data S-12

S6. LPS Discrimination and Classification S-14

S7. Antimicrobial Peptide Properties S-18

S1. Surface Derivitization Reactions for RAIRS characterization

Surface derivitization reactions for IR characterization proceeded as follows. The mixed OEG-SAM was placed into a custom sample holder and 200 μL of a 25 mM solution of *N*-[γ-maleimidobutyryloxy]sulfosuccinimide ester (sulfo-GMBS) in 0.1 M borate buffer, pH 8.5 was placed on top. The surface was incubated at room temperature for 20 minutes after which the surface was removed, rinsed with deionized H_2O, and dried with UHP N_2. RAIR spectra were collected to verify the presence of new terminal maleimide moieties and the surface was placed back into a new well of the custom sample holder. A 200 μL aliquot of a 10 mM solution of the desired peptide in 0.1 M PBS, pH 6.5 was placed on top of the slide for 1 to 20 hours at room temperature. The surface was then removed, rinsed with the same PBS followed by DI H_2O and dried with UHP N_2. RAIR spectra were immediately recorded. Vibrational mode assignments were made via literature precedent as outlined in the text.

S2. Peptide Immobilization on SPR Substrates

For each new surface, the system was first primed with running buffer (PBS pH 6.5). Next, the detector response was normalized to all four flow channels using the glycerol containing normalization solution provided by Biacore. After normalization, ligands were independently immobilized to each flow channel as follows. First, 50 mM sulfo-GMBS dissolved in 0.1M borate buffer, pH 8.5 was injected for 240 seconds at a flow rate of 10 μL/min. Sulfo-GMBS reacts with the terminal primary amine groups of the mixed SAM to form a stable amide linkage connected to a new terminal maleimide

moiety, which is subsequently used to covalently bind the thiol groups of terminal cysteine residues via the formation of thioether bonds.[9] For the cysteine reference ligand in flow channel 1, 50 mM cysteine dissolved in running buffer was next injected for 240 seconds. For the peptide ligands in channels 2-4, the peptide solution was injected using the Target RU command of the Biacore software, which instructs the instrument to inject ligand solution in small volume pulses at 5 μL/min until a preset immobilization RU value is reached. After the target is reached, 50 mM cysteine is injected for 240 seconds at 10 μL/min to passivate any unreacted maleimide groups. The flow channels were always immobilized in numerical order.

S3. LPS Binding

Quantification of LPS binding to each peptide was determined using a custom method with 0.1M phosphate buffer, pH 7.4 containing 137 mM NaCl and 0.01% P20 surfactant as the running buffer. The first three cycles were conditioning cycles where buffer was used as the injected analyte instead of LPS. These initial cycles help equilibrate the surface and remove any loosely bound material from the surface. LPS samples were divided into two sets; a training set and a validation set. Each set was prepared independently from the same 1 mg/mL stock LPS solutions. Beginning with cycle 5, the LPS training data set was analyzed in sequential order with four replicate measurements per five LPS samples for a total of 20 cycles. The four replicates of each LPS were analyzed sequentially. The validation set was analyzed next, but in random order, again with 4 replicates per five LPS samples. Each injection cycle proceeded as follows: First, the 10 μg/mL LPS sample is injected over all four flow channels (in order from 1 to 4) at 10 μL/min for 300 seconds after which the flow is reverted back to running buffer. After a dissociation time of 120 seconds, the surface is regenerated using a solution of 50 mM NaOH with 30% acetonitrile and 0.1% Tween 20 surfactant injected for 30 seconds at a flow rate of 50 μL/min. An injection of running buffer follows for 30 seconds at 50 μL/min to remove the basic regeneration solution from the surface. The system is then allowed to equilibrate with running buffer for six minutes before moving on to the next cycle. The amount of bound LPS is determined by

measuring the binding response five seconds after the termination of sample injection. The slight delay in measurement allows the response to adjust for any bulk refractive index differences between the running buffer and sample solutions. All of the responses reported have been reference subtracted, i.e the response of the reference cysteine channel (FC1) has been subtracted from the response of the ligand channel (FC2,3,4). The response of the reference channel also serves as a negative control to monitor non-specific binding.

S4. Correction for Peptide Binding Affinity Decay

Despite no observation of a decrease in immobilized peptide density, the binding of LPS decreased as a function of time. This phenomenon is known to the SPR biosensing community and was addressed by Ober et al. where they corrected for the time-dependent response decay using an exponential function applied to kinetic data. The time-dependent decrease of peptide binding affinity in our system is deleterious to linear discriminant analysis based classification as significant within-group variation leads to poor discrimination. A method was therefore developed and modeled after the aforementioned study by Ober et al. to correct for peptide activity loss by following the response of a control analyte throughout the course of the entire experiment. The control data set for each of the three peptides was fit with a unique exponential decay function. The measured binding response at a particular cycle number (time) was corrected by a factor determined by the ratio of the maximum response at the initial time to the calculated response determined by the fitting function. Figure S1 shows the time-dependent response of 10 μg/mL LPS from *E. coli* O111:B4 to immobilized SMAP-29 along with the exponential decay fit and the resultant corrected data. The binding decay is a consequence of peptide activity loss and not LPS activity loss as injecting a freshly prepared LPS sample after the presented analysis resulted in a similar binding response to that of latter cycles (>40), indicating that the activity loss is peptide dependent. Further evidence for the lack of peptide loss is shown in Figure S3 where the absolute instrument baseline of each immobilized peptide channel was monitored as a function of cycle number.

The absence of significant baseline decrease supports the assumption of minimal peptide desorption during the experiment.

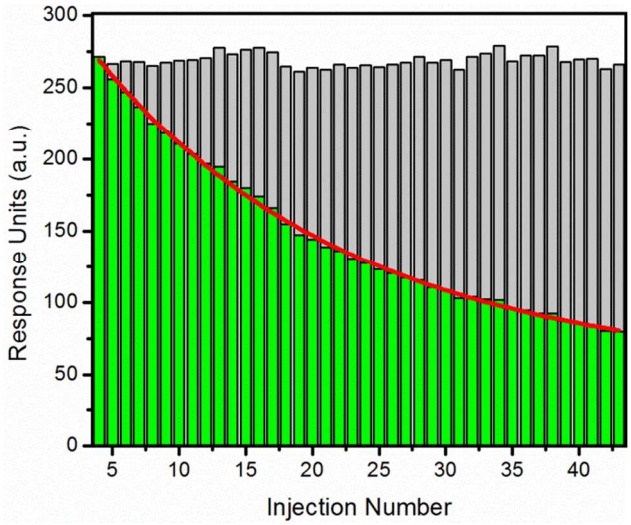

Figure S1: Binding response of 10 µg/mL LPS from E. coli O111:B4 to immobilized SMAP-29 as a function of injection number. The green bars are the raw data and the grey bars are the same data corrected to the exponential decay function (red trace) fit to the raw data.

The binding activity of the peptides was observed to decay as a function of cycle (or time) independent of LPS activity. To correct for the peptide activity loss, a control data set was collected where regular measurements of *E. coli* O111:B4 LPS binding to the three immobilized peptides were collected over the course of the entire experiment. Figure S2 below shows the binding of the control LPS to the three peptides. The response of each peptide was fit to an exponential decay of the type $y = A_1 * \exp\left(-x/t_1\right) + y_0$.

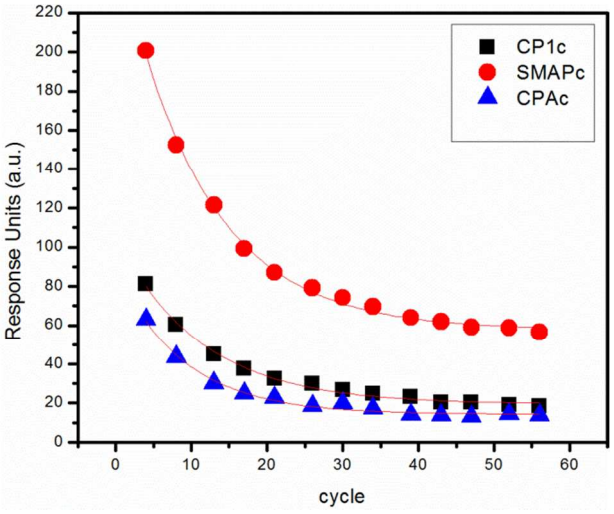

Figure S 2: Binding of 10 ug/mL LPS of E. coli O111:B4 as a function of cycle number (time).

Model	ExpDec1		
Equation	y = A1*exp(-x/t1) + y0		
Reduced Chi-Sqr	2.07351	5.27618	2.15997
Adj. R-Square	0.99402	0.99719	0.98984
		Value	Std. Error
CP1c	y0	19.43542	0.78501
	A1	86.72272	2.68175
	t1	11.11162	0.6113
SMAPc	y0	57.69456	1.24754
	A1	202.2681	4.29448
	t1	11.06744	0.41657
CPAc	y0	14.2407	0.66732
	A1	75.12133	3.45846
	t1	8.86338	0.6061

Table S 1: Exponential decay fit parameters for the data in Figure S1.

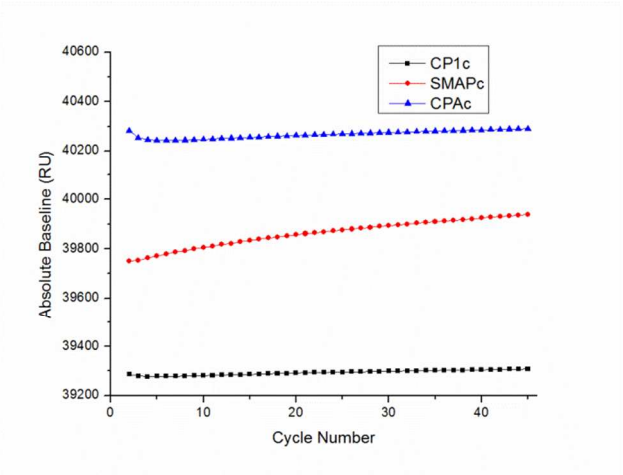

Figure S3: Plot of the absolute baseline response versus cycle number for the three antimicrobial peptides CP1c, SMAPc, and CPAc. The slightly increasing baseline over time supports the assumption of little to no peptide desorption during the experiment.

To verify that a single LPS strain could be used for the activity decay correction of all the LPS molecules tested, a separate experiment was performed to verify the similar activity decay profiles of all the LPS. Briefly, each of the five LPS strains was tested for binding over binding a total of ten times in sequential order (LPS 1,2,3,4,5,1,2,3,4,5,..,). To compare the activity decay, plots of the natural log of the cycle number versus the natural log of the uncorrected binding for each LPS strain were prepared; these plots are seen in Figure S4. For each peptide, the log-transformed decay profiles of each LPS are visually similar, suggesting that the time dependent binding activity loss is a function of the peptide and not the LPS. Furthermore, these data justified the use of a single LPS strain for monitoring the binding activity decay of every LPS strain.

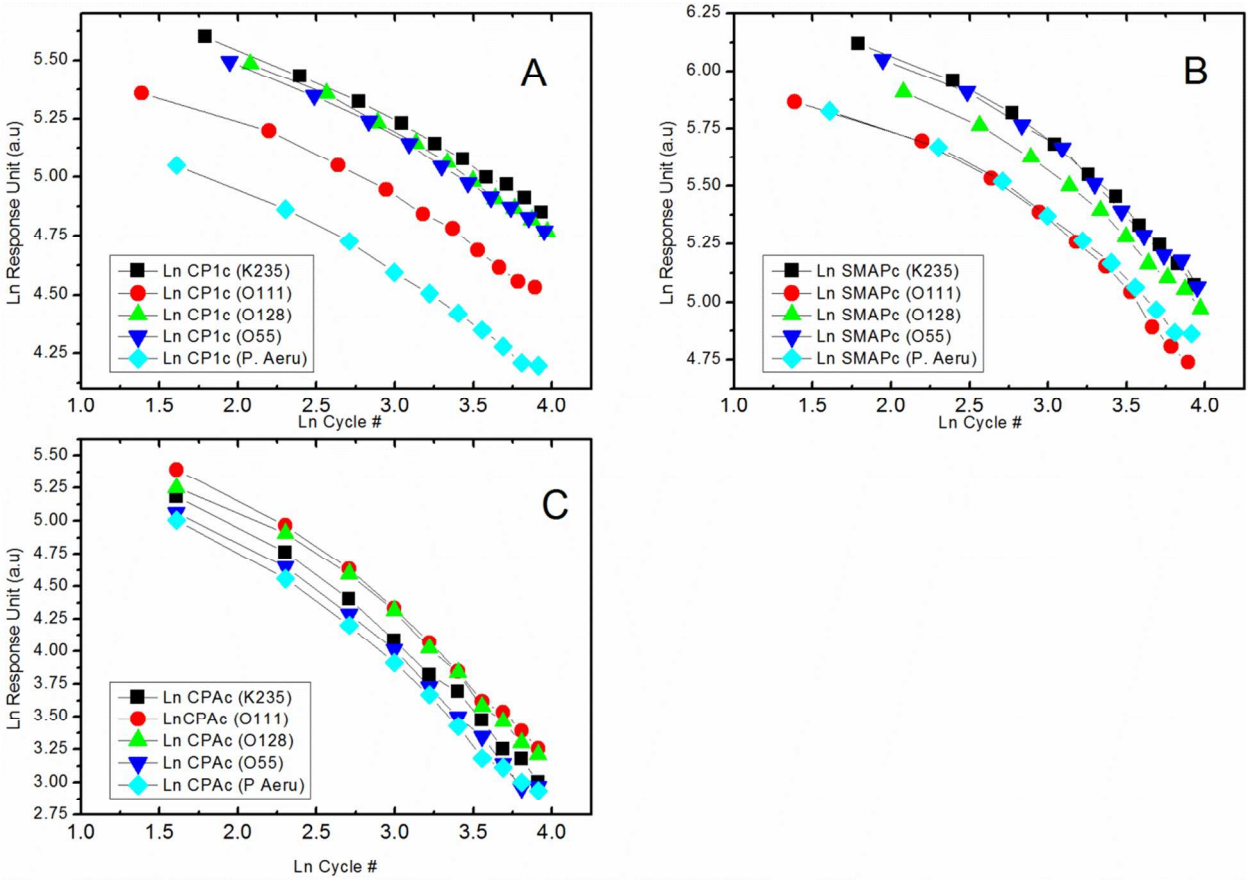

Figure S 4: Natural log plots of cycle number (time) versus binding for the five LPS strains to the three immobilized AMPS; A) CP1c, B) SMAPc, and C) CPAc.

S5. Peptide-LPS Binding Decay Correction Data

The data used for discrimination was corrected for peptide binding activity decay as described above. Table S2 shows the raw uncorrected data and the corresponding corrected data along with pertinent statistics.

LPS	CP1c Avg	CP1c RSD	SMAPc Avg	SMAPc RSD	CPAc Avg	CPAc RSD
K235 A	46.06	8.00%	87.35	12.72%	25.58	9.83%
K235 A*	95.90	1.75%	170.15	5.73%	64.27	5.22%
K235 B	29.67	11.14%	42.07	6.11%	13.41	8.78%
K235 B*	94.76	6.13%	132.12	2.64%	55.09	6.15%
O111 A	64.37	13.52%	158.03	11.23%	46.37	11.52%
O111 A*	76.52	3.05%	185.98	1.67%	57.69	2.40%
O111 B	20.83	8.79%	65.76	1.17%	14.95	6.35%
O111 B*	81.82	7.64%	218.56	1.88%	64.03	6.25%
O128 A	37.73	4.84%	70.19	4.97%	19.12	11.81%
O128 A*	111.86	3.07%	185.57	1.50%	66.72	9.40%
O128 B	22.53	14.09%	59.39	10.45%	12.14	27.01%
O128 B*	98.96	7.92%	184.06	5.52%	49.06	23.23%
O55 A	32.48	7.41%	64.71	1.73%	20.54	6.80%
O55 A*	83.05	2.74%	151.35	3.59%	62.39	1.24%
O55 B	22.40	14.59%	43.74	12.74%	14.52	19.60%
O55 B*	82.10	8.13%	137.50	7.09%	59.50	16.32%
P. aeru A	22.83	10.59%	101.48	5.15%	27.97	7.29%
P. aeru A*	41.41	2.94%	157.44	3.30%	50.55	4.94%
P. aeru B	12.49	13.69%	60.18	11.65%	16.36	17.50%
P. aeru B*	44.61	6.50%	185.41	5.17%	65.85	12.96%

Table S 2: Raw and corrected LPS binding data. The data are the average of four replicate measurements along with the percent relative standard deviation (RSD; standard deviation/average). For each data set, the asterisk-labeled set was corrected using the described decay correction process.

S6. LPS Discrimination and Classification

LPS samples were classified using the corrected binding data subjected to linear discriminant analysis. The classification functions were generated using corrected Data Set A, which was collected in sequential order first. The classification was then verified using corrected Data Set B subjected to the classification functions generated from Data Set A. Table S3 below shows the Mahalanobis distances of each data point to the centroid of each LPS strain. The data point was assigned to the strain with the shortest distance. Red shaded cases were misclassified.

Group	Case	Data Set	K235	O111	O128	O55	P aeru
K235	1	A	8.217	116.398	20.851	129.675	868.008
	2	A	2.012	75.608	56.992	65.488	709.017
	3	A	3.687	108.101	44.196	75.883	776.32
	4	A	3.383	102.242	58.198	65.055	744.177
	21	B	40.421	189.377	90.303	91.34	843.023
	22	B	58.052	175.187	127.428	73.783	757.365
	23	B	50.435	130.104	145.237	38.123	642.575
	24	B	51.302	146.21	137.481	49.323	684.388
Group	**Case**		**K235**	**O111**	**O128**	**O55**	**P aeru**
O111	5	A	80.786	0.903	203.923	47.45	398.754
	6	A	95.853	0.111	231.937	46.153	361.27
	7	A	103.834	0.341	238.655	53.955	359.007
	8	A	106.744	0.814	252.593	41.714	331.393
	25	B	70.566	73.317	110.035	168.169	730.723
	26	B	90.018	47.854	152.894	152.178	624.951
	27	B	167.505	59.756	271.02	187.472	526.259
	28	B	146.709	53.625	227.074	186.493	568.45
Group	**Case**		**K235**	**O111**	**O128**	**O55**	**P aeru**
O128	9	A	27.113	191.789	2.558	198.762	1,057.28
	10	A	51.124	263.924	2.088	256.437	1,209.73
	11	A	48.384	254.748	1.401	250.884	1,192.82
	12	A	49.778	227.94	7.415	231.099	1,124.72
	29	B	31.793	167.086	9.697	192.291	1,004.71
	30	B	51.811	197.915	13.898	229.094	1,072.85
	31	B	47.982	132.01	49.296	161.477	872.535
	32	B	107.074	235.983	70.32	259.851	1,072.86
Group	**Case**		**K235**	**O111**	**O128**	**O55**	**P aeru**
O55	**13**	A	85.592	65.303	239.907	1.636	402.133
	14	A	57.801	55.508	191.37	2.543	451.043
	15	A	81.422	35.987	232.907	0.898	368.652
	16	A	101.532	37.85	267.083	2.469	329.296
	33	B	96.034	70.809	257.941	3.157	388.777
	34	B	68.521	85.051	207.906	9.275	479.102
	35	B	124.253	91.492	302.385	10.494	368.199
	36	B	130.816	103.914	290.693	20.757	401.759
Group	**Case**		**K235**	**O111**	**O128**	**O55**	**P aeru**
P. aeru	**17**	A	748.873	352.732	1,117.58	366.638	1.101
	18	A	733.483	342.771	1,100.81	356.503	0.914
	19	A	799.355	377.299	1,175.14	410.115	0.75
	20	A	803.034	379.976	1,182.08	414.846	1.759
	37	B	872.949	423.827	1,260.94	492.574	37.281
	38	B	951.758	477.864	1,355.82	547.827	39.673
	39	B	832.412	399.072	1,213.22	463.436	38.645
	40	B	740.634	327.704	1,099.56	385.835	10.14

Table S 3: Calculated Mahalanobis distances of each data point from the centroid of each group (LPS strain). Misclassified cases are outlined and shaded in red.

Table S4 shows the group classification of each data point based on the Mahalanobis distances.

Training Data Classification (Set A) (cases in row categories classified into columns)

	K235	O111	O128	O55	P AERU	%correct
K235	4	0	0	0	0	100
O111	0	4	0	0	0	100
O128	0	0	4	0	0	100
O55	0	0	0	4	0	100
P AERU	0	0	0	0	4	100
Total	4	4	4	4	4	100

Jackknifed Verification Data (leave-one-out method)

	K235	O111	O128	O55	P AERU	%correct
K235	3	0	1	0	0	75
O111	0	4	0	0	0	100
O128	0	0	4	0	0	100
O55	0	0	0	4	0	100
P AERU	0	0	0	0	4	100
Total	3	4	5	4	4	95

Verification Data Classification (Set B)

	K235	O111	O128	O55	P AERU	%correct
K235	2	0	0	2	0	50
O111	1	3	0	0	0	75
O128	1	0	3	0	0	75
O55	0	0	0	4	0	100
P AERU	0	0	0	0	4	100
Total	4	3	3	6	4	80

Table S 4: Group classifications of each data point. The training data set (Set A) was used to generate classification functions and the Validation Set (dataset B) was used to test the classification functions on independent data. The jackknifed data generates classification functions for each data point while leaving the tested data out.

S7. Antimicrobial Peptide Properties.

The natural antimicrobial peptides used in our study exhibit different physical and chemical properties which we hypothesize to be responsible for their discriminatory binding capabilities. Table S5 lists the reported and calculated values of some of these properties.

Name	Charge	Hydrophobicity	Hydrophobic Moment	Polar%	Non-polar %	Spatial Charge Density	Spatial Hydroph. Density	Spatial Denisty Ratio
CP1c	5	0.231	0.256	59.38%	40.63%	128.155	343.852	2.683
SMAPc	9	0.331	0.441	53.33%	46.67%	257.659	294.700	1.144
CPAc	6	0.319	0.234	47.22	52.78	222.585	448.786	2.016
cCP1	5	0.231	0.247	59.38%	40.63%	101.175	350.042	3.460

Table S 5: Select properties of immobilized antimicrobial peptides. See supplemental text for descriptions.

The charge, hydrophobicity, hydrophobic moment, polar and non-polar% were obtained via the online HeliQuest software available at http://heliquest.ipmc.cnrs.fr. The last three properties were calculated by us and are dependent on peptide immobilization orientation, the explanation of which is aided by Figure S4. Individual residues are assigned an increasing numerical value dependent on distance from the surface. For the charge density calculation, a cationic residue is assigned a value of 1, an anionic residue -1, and a neutral residue 0. The charge-assigned value is then multiplied by the distance dependent numerical value, resulting in charged residues further from the surface having a higher charge density value than those closer to the surface. The sum of the charge density values for each residue of the sequence is then taken to provide the overall spatial charge density. The spatial hydrophobicity is determined similarly, but rather than assigning 1,-1, or 0, the unique hydrophobicity of each residue (determined by Black and Mould) is used and multiplied by the same distance dependent numerical value. The spatial density ratio is simply the ratio of the spatial hydrophobicity to the spatial charge density. The trend is that peptides with charge localized closer to the solution will have smaller ratios than those with charge closer to the surface.

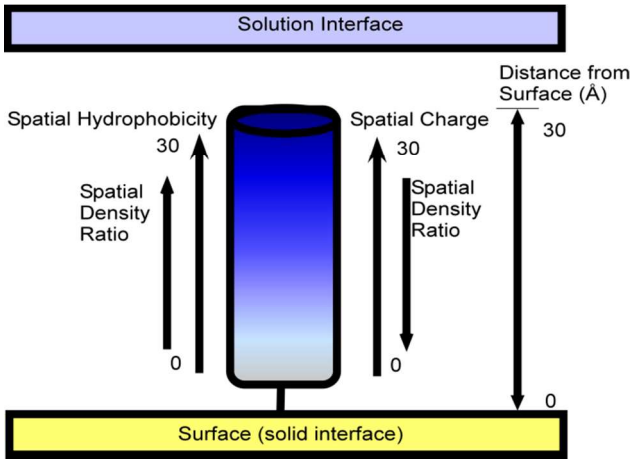

Figure S 4: Graphical representation of the spatially dependent physiochemical properties used to analyze LPS binding. A peptide molecule, represented by the blue cylinder, is attached to a solid surface and extends into the solution interface. The spatial dependent charge and hydrophobicity of an individual residue increase as it gets farther from the solid interface and closer to the solution interface. The spatial density ratio is directly proportional to the spatial hydrophobicity and inversely proportional to the spatial charge.